

# THE INFLUENCE OF EQUATORIAL WAVES ON QUIKSCAT WINDS IN THE ATLANTIC

Paulo S. Polito<sup>1</sup>, Olga T. Sato<sup>1</sup> and W. Timothy Liu<sup>2</sup>

<sup>1</sup> Earth Observation Department  
INPE - National Institute for Space Research, Brazil

<sup>2</sup> Jet Propulsion Laboratory  
California Institute of Technology

## INTRODUCTION

Scatterometer measurements depend on the sea surface roughness which is in principle caused by the **wind stress against a static ocean surface**.

Alternatively, a **moving ocean against the static atmosphere** can have the same effect. [4] has shown that currents linked to Tropical Instability Waves (TIWs) induce a signal in the scatterometer winds in the eastern tropical Pacific.

This study investigates the hypothesis that surface currents associated with TIWs and equatorial Rossby waves can **bias the QuikScat scatterometer winds** in the region of the **PIRATA** buoys in the Atlantic.

## THEORY

**TIWs are Rossby-gravity waves** generated by barotropic instability. These waves are seasonally and interannually modulated by equatorial currents.

TIWs zonal phase speed ( $c_p$ ), wavelength ( $\lambda$ ) and period ( $P$ ) are on the order of **-35 km day<sup>-1</sup>, 1000 km and one month** [6]. These attributes can vary by more than a factor of 2.

1<sup>st</sup> order theory indicates zonal propagation thus meridional geostrophic **currents**  $v_g$  arise associated with the **slopes** of the surface.

$$v_g = \frac{g}{f} \frac{\partial \eta}{\partial x}, \quad (1)$$

Geostrophy does not apply at (or at few degrees of) the equator because  $f$  is evanescent.

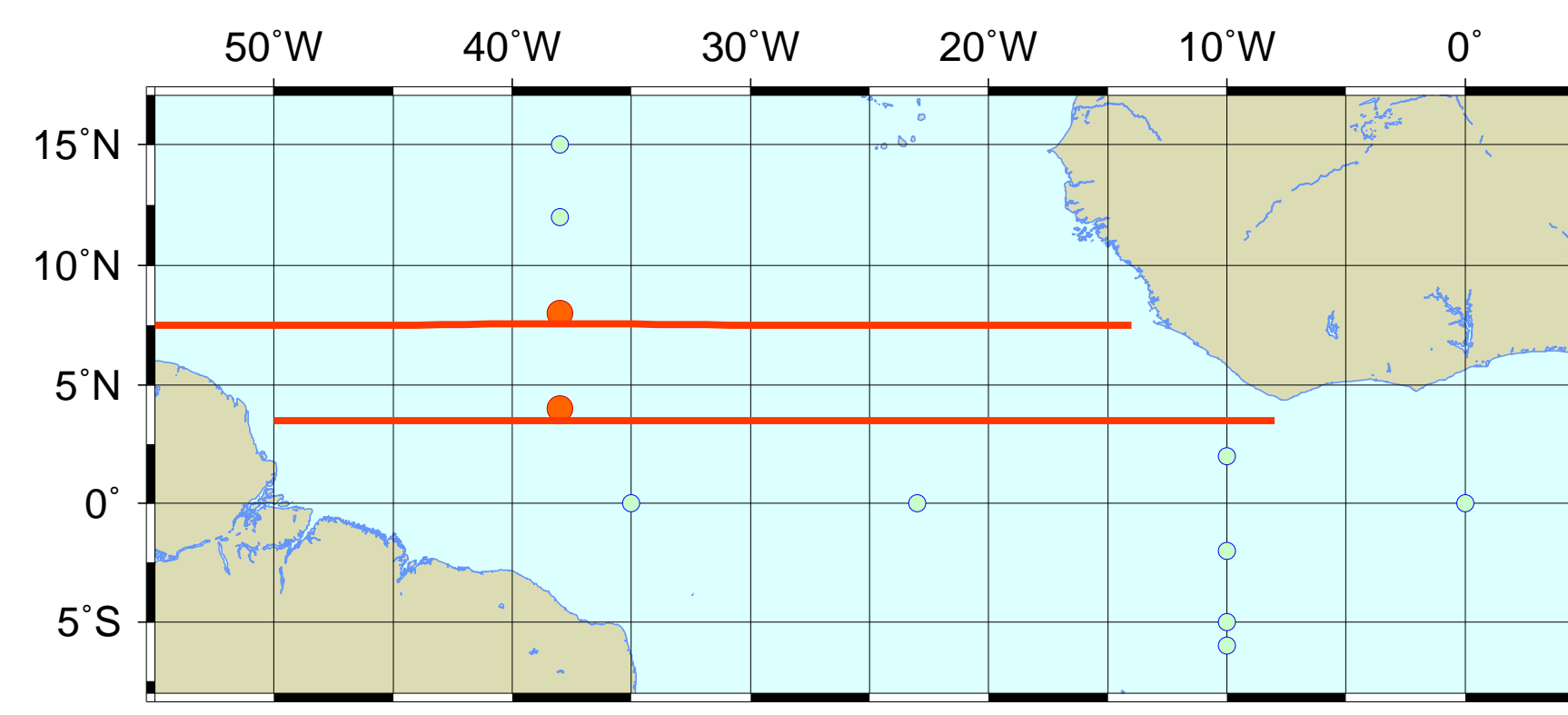


Figure 1: Pilot Research Moored Array in Tropical Atlantic (PIRATA) buoys (circles) and TOPEX/POSEIDON (T/P) altimetry tracks (lines). Locations studied in detail are red, others are blue.

## METHODS

**WINDS** The **in-situ** winds  $v_{pi}$  between 3/00 and 5/01 are daily averages of PIRATA buoy measurements, available on-line.

The  $12h \times 1/4^\circ$  interpolated **QuikScat** winds  $v_{qs}$  are distributed by JPL/PODAAC.

The **difference**  $\Delta v = v_{pi} - v_{qs}$  between meridional wind components from **PIRATA** and **QuikScat** measurements is calculated from winds that are measured in the **same day** and are up to **28 km** apart.

$v_{pi}$  and  $v_{qs}$  are referred to heights of **4 and 10 m**.  $v_{pi}$  is multiplied by a constant such that the corrected  $v_{pi}$  explains the most variance from  $v_{qs}$ .

**HEIGHT** The waves are detected by the T/P altimeter in the PIRATA region. The corrected sea surface height anomaly  $\eta$  is calculated in relation to an 8-year average (1993–2000), is bicubically interpolated to a  $1^\circ \times 1^\circ$  grid and stored as  $\eta_o(x, t)$ .

**Finite impulse response filters** decompose  $\eta_o(x, t)$  into spectral bands associated with:

- $\eta_t$  → Basin-wide, non-propagating signal (mostly seasonal)
- $\eta_{24,12,6,3}$  → Long 1<sup>st</sup> mode **Rosby waves** ( $P = 24, 12, 6$  and 3 months)
- $\eta_1$  → **Tropical instability waves** ( $P = 1.5$  months)
- $\eta_{K6,K3,K1}$  → Equatorial Kelvin waves ( $P = 6, 3$  and 1.5 months)
- $\eta_{E,r}$  → meso-scale eddies and a small scale residual

$$\text{i.e.: } \eta_o = \eta_t + \eta_{24} + \eta_{12} + \eta_6 + \eta_3 + \eta_1 + \eta_{K6} + \eta_{K3} + \eta_{K1} + \eta_E + \eta_r. \quad (2)$$

This method is described in detail in [5].

The **meridional current**  $v_g$  is estimated based on the filtered T/P components  $\eta_3$  and  $\eta_1$ , (smaller  $L \Rightarrow$  stronger currents).

**COMPARISON**  $\Delta v$  is **smoothed** with a spline-based routine whose tension is adjusted to maximize their cross-correlation  $c$  with  $v_g$ .

$c$  is calculated for all buoys and its statistical significance is obtained by Monte Carlo simulations based on the number of **original** T/P samples.

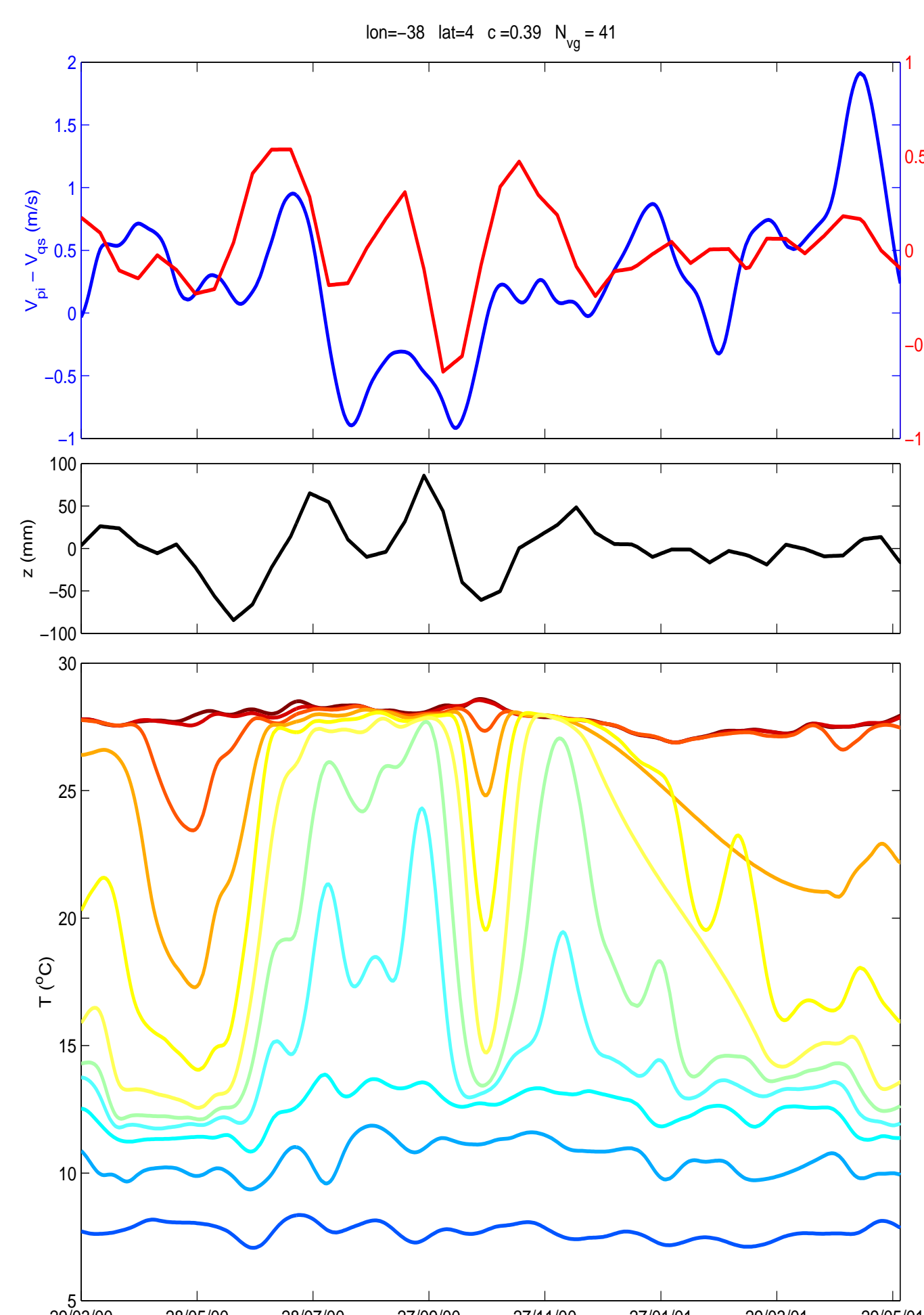


Figure 2: Results from QuikScat, TOPEX/POSEIDON and the PIRATA buoy at 38° W, 4° N.

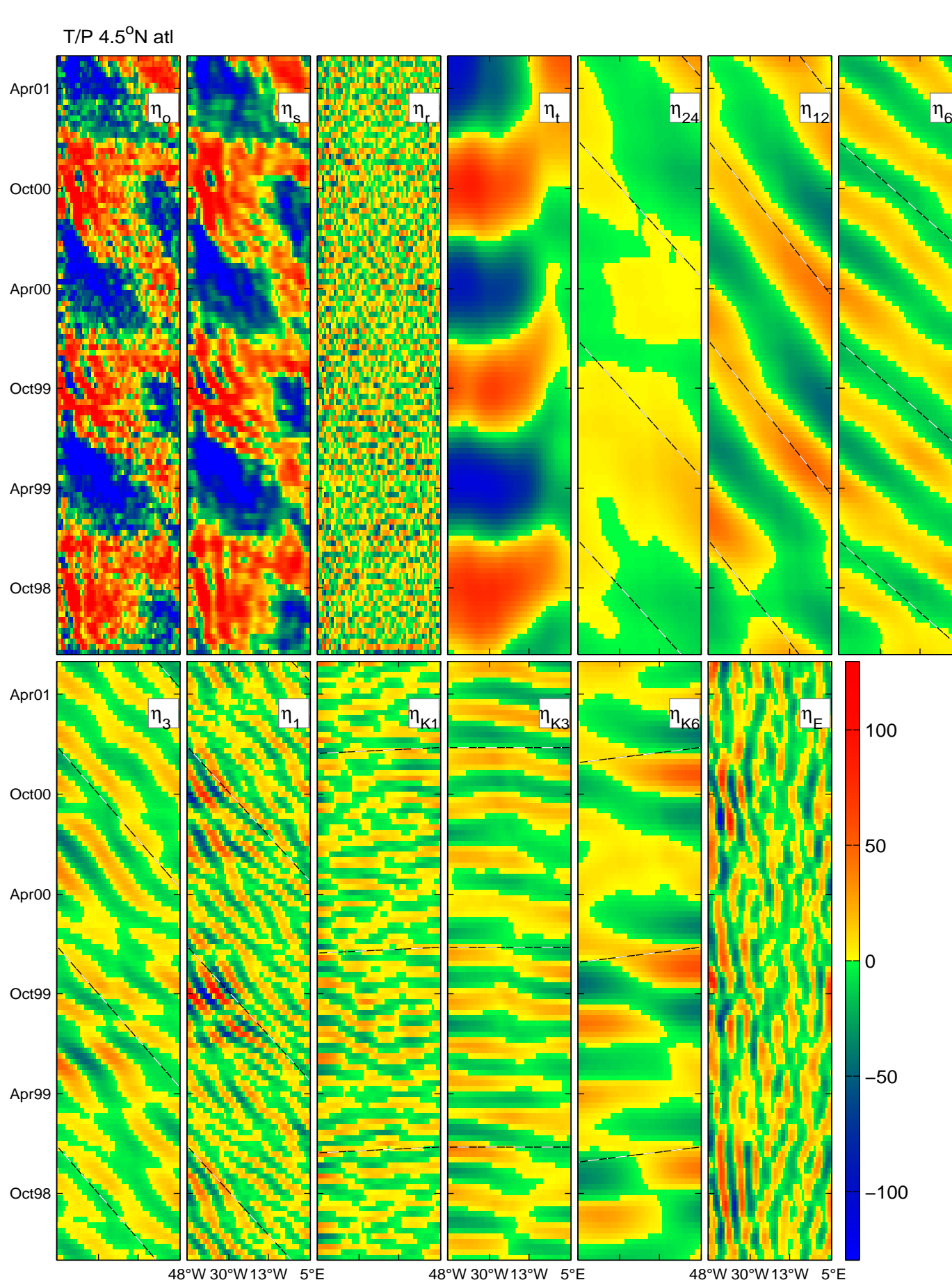


Figure 3: Original ( $\eta_o$ ), sum of filtered ( $\eta_s$ ), residual ( $\eta_r$ ), and filtered sea surface height anomaly fields ( $\eta_t, \eta_{24}, \eta_{12}, \eta_6, \eta_3, \eta_1, \eta_{K1}, \eta_{K3}, \eta_{K6}$  and  $\eta_E$ ), as in Equation 2 at 3.5° N in the Atlantic, in mm. Dash-dot lines are estimates for mean zonal phase speed.

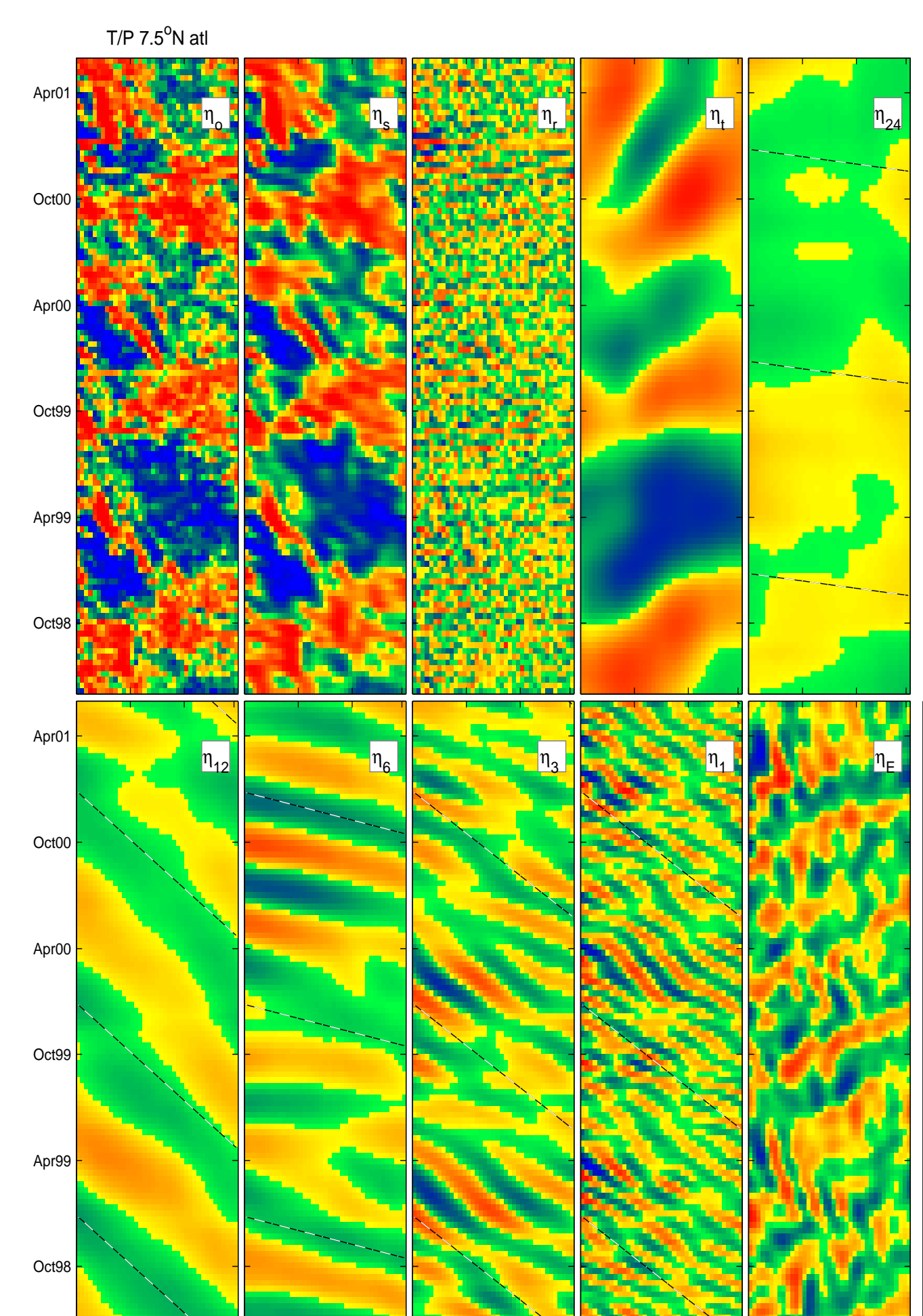


Figure 4: Same as Figure 3 but for 7.5° N.

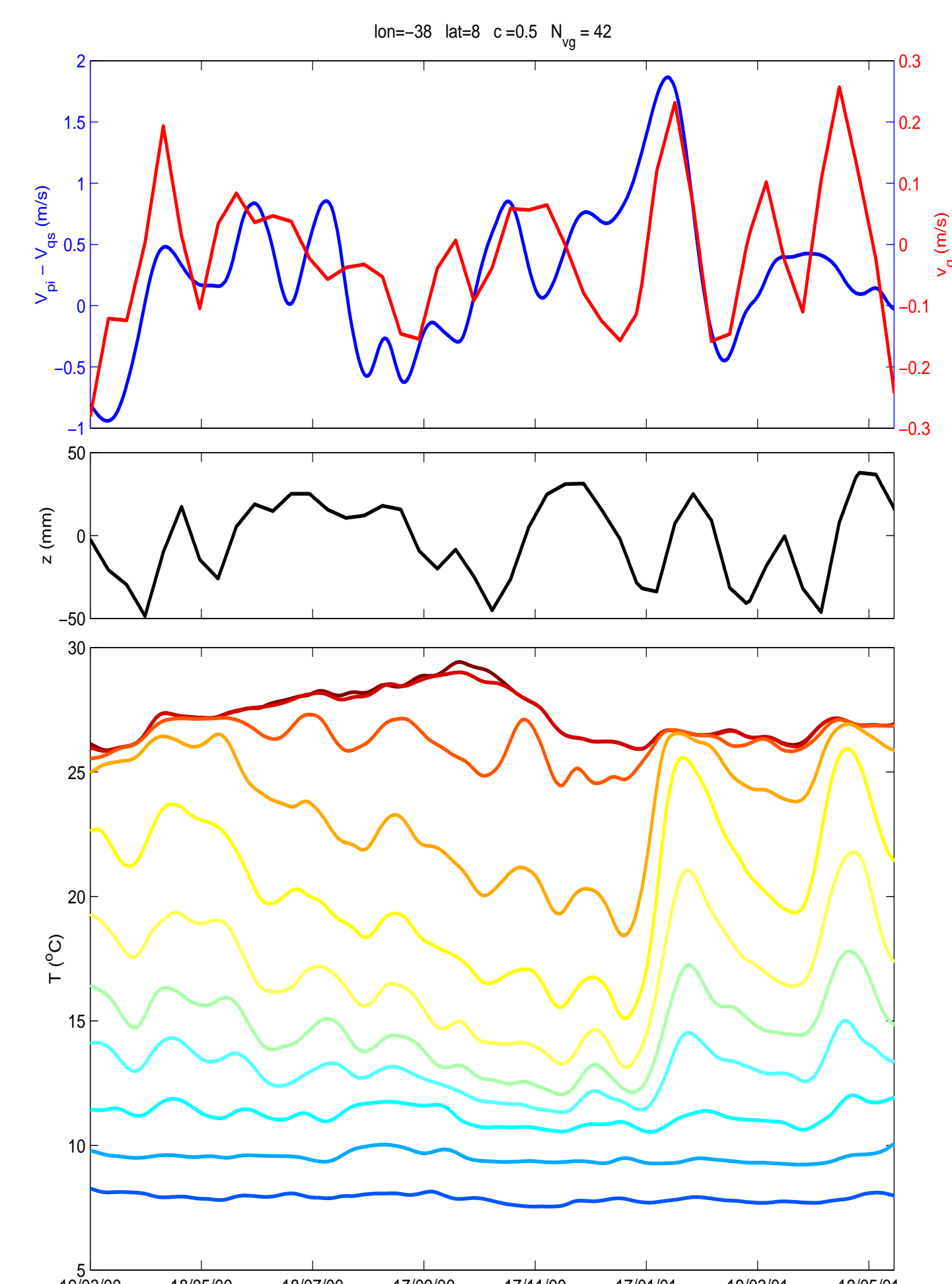


Figure 5: Results from QuikScat, TOPEX/POSEIDON and the PIRATA buoy at 38° W, 8° N.

## RESULTS

Longitude	Latitude	$c$	$N_{vg}$
0°	0°	.17	25
10° W	0°	-.06	28
10° W	2° S	-.31	9
10° W	5° S	-.75	11
10° W	6° S	.03	42
10° W	10° S	-.04	29
10° W	2° N	.42	9
23° W	0°	.34	44
35° W	0°	.18	37
<b>38° W</b>	<b>4° N</b>	<b>.39</b>	<b>41</b>
<b>38° W</b>	<b>8° N</b>	<b>.50</b>	<b>42</b>
38° W	12° N	-.07	46
38° W	15° N	-.31	20

**Table 1** shows the correlation  $c$  and the number of

original T/P samples  $N_{vg}$ . The 2 buoys in bold are the red circles in Figure 1, selected because they **(1)** have long time series, **(2)** are far from the equator and **(3)**  $c$  is statistically significant at a 95% confidence level.

In **Figure 2** the top plot shows the positive correlation between  $\Delta v$  and  $v_g$ . The middle plot shows sea surface height anomaly associated with trimestral Rossby waves ( $\eta_3$ ) and TIWs ( $\eta_1$ ). The bottom plot shows temperature time series for thermistors at 1, 20, 40, 60, 80, 100, 120, 140, 180, 300 and 500 m, from red to blue.

The **magnitude** of  $v_g$  is similar to that of  $\Delta v$ .

**Figure 3** shows a dominant seasonal signal  $\eta_t$  and very clear annual and semiannual Rossby waves ( $\eta_{12}, \eta_6$ ). Kelvin wave components ( $\eta_{K1}, \eta_{K3}$ , and  $\eta_{K6}$ ) are not well defined. **TIWs** ( $\eta_1$ ) show energetic bursts on October of 1999 and 2000. The **trimestral Rossby waves** ( $\eta_3$ ) bursts occur approximately two months

earlier.

$\eta_3$  and  $\eta_1$  have average phase speeds (-23 and -24 km/day), periods (124 and 57 days) and wavelengths (2852 and 1368 km) within the expected range. The TIW signal that T/P can capture is on the low-frequency end of the TIW spectrum, due to its **10 day sampling rate**.

A stronger argument comes from the buoy at 38° W, 8° N, **Figure 5**.  $c$  is larger than at 38° W, 4° N although  $\Delta v$  (top, blue line) shows more variability than the T/P-derived  $v_g$  (red line). This is probably due to the **sampling rate difference**. The PIRATA data, particularly the yellow and green curves between 60 and 100 m in 1999 and 2000, show wave-like variability with  $\sim$  one month period, a signal not fully captured by the T/P altimeter.

In **Figure 4** the  $\eta_1$  signal shows pulses of high amplitude centered approximately on March of 1999,

2000 and, with less intensity, 2001. The  $\eta_3$  signals occur approximately one month earlier.

The bottom plots of Figures 2 and 5 show the vertical structure of Rossby waves and TIWs. The surface layer (1 m, dark red) temperature variability is **dominated by the seasonal signal**, while the variability at the frequency bands of  $\eta_3$  and  $\eta_1$  has an amplitude of a **fraction of a degree**. The amplitude of the wave-like temperature signal at 80 m is **up to 7° C** in 2001.

## CONCLUSIONS

**Significant correlations** between  $\Delta v$  and  $v_g$  are observed at 4° N, 38° W and 8° N, 38° W.

At these two latitudes **TIWs are very clear** in the filtered T/P record. The PIRATA temperature profiles corroborate these observations.

The presented evidences suggest that a significant part of the wind difference is **not random**. Instead, it is a **bias** introduced by ocean currents associated with TIWs and Rossby waves.

The alternative hypothesis to explain the influence of TIWs in the wind is based on the **enhanced vertical mixing and depends on sea surface temperature anomalies** ([7],[2], and later [1], [3]).

Figures 2 and 4 show that the **SST variability is weak** and surpassed by that of the sub-surface layer by one order of magnitude. These evidences suggest that this hypothesis does not hold in the 2 selected buoy locations.

Although scatterometer winds are probably biased by the surface currents, the scatterometer **stress** is correct and includes the contribution from the moving ocean surface.

e-mail for contact: [polito@tid.inpe.br](mailto:polito@tid.inpe.br)

## References

- [1] D. B. Chelton, F. J. Wentz, C. L. Gentemann, R. A. de Szoeke, and M. G. Schlax. Satellite microwave sst observation of transequatorial tropical instability waves. *Geophysical Research Letters*, 27:1239–1242, 2000.
- [2] S. P. Hayes, M. J. McPhaden, and J. M. Wallace. The influence of sea surface temperature on surface wind in the eastern equatorial Pacific. *Journal of Climate*, 2:1500–1506, 1989.
- [3] W. T. Liu, X. Xie, P. S. Polito, S.-P. Xie, and H. Hashizume. Atmospheric manifestation of tropical instability wave observed by QuikSCAT and Tropical Rain Measuring Mission. *Geophysical Research Letters*, 27:2545–2548, 2000.
- [4] P. S. Polito, J. P. Ryan, W. T. Liu, and F. P. Chavez. Oceanic and atmospheric anomalies of tropical instability waves. *Geophysical Research Letters*, 28(11):2233–2236, 2001.
- [5] P. S. Polito, O. T. Sato, and W. T. Liu. Characterization and validation of heat storage variability from Topex/Poseidon at four oceanographic sites. *Journal of Geophysical Research*, 105(C7):16911–16921, 2000.
- [6] L. Qiao and R. H. Weisberg. Tropical instability wave kinematics: observations from the tropical instability wave experiment (TIWE). *Journal of Physical Oceanography*, 100:8677–8693, 1995.
- [7] J. M. Wallace, T. P. Mitchell, and C. Deser. The influence of sea surface temperature on surface wind in the eastern equatorial Pacific: Seasonal and interannual variability. *Journal of Climate*, 2:1492–1499, 1981.